

## Effects of damage build-up in range profiles in crystalline Si; molecular dynamics simulations

J. Peltola, K. Nordlund and J. Keinonen

Accelerator Laboratory, P.O. Box 43, FIN-00014 University of Helsinki, Finland  
(September 28, 2001)

Molecular dynamics has been successful in predicting range profiles for ions implanted into crystalline materials in the dose regime where it can be approximated that changes in the sample structure do not affect the profiles. Many experimental distributions are, however, strongly dose-dependent due to the amorphization of the crystalline material. This has so far been taken into account only in some binary-collision-approximation calculations with a damage build-up model that depends on the probability for the amorphization to occur at a certain depth. We present here a fast molecular dynamics model for predicting range profiles of ions in crystalline Si. The model includes cumulative damage build-up, where the amorphization states are taken from molecular dynamics simulations of cascade damage. The method can be used to predict profiles for any material. We used silicon because of the large amount of experimental data available. No free parameters were used. Comparison of results to a wide range of experiments show very good agreement.

PACS numbers: 61.72.Tt,61.85.+p,34.50.Bw,34.10.+x

**Keywords:** Ion implantation, range profile, damage, semiconductors

### I. INTRODUCTION

The continuing demand for better components in silicon based ion-implantation technology requires smaller component sizes and more accurate knowledge about implantations<sup>1</sup>. One major interest is the implantation profiles of ions. This is related to the technical performance of a device. Lower implantation energies are needed for smaller device sizes and accurate profiles in a crystalline material can not be obtained without knowledge of channeling effects. Damage that accumulates into the crystal structure during the implantation process, changes the channeling probability along with the dose. This implies that modeling of the damage build-up process is of importance, especially in high-dose implantations where the material can turn totally amorphous in the implanted region.

The computer simulation models for predicting range profiles in crystalline materials have traditionally been based on two different techniques, namely Monte Carlo (MC)/ Binary-Collision-Approximation (BCA) and Molecular Dynamics (MD) techniques. In a conventional MC method the positions of atoms which a recoiling ion is about to collide with, are randomly chosen. Thus these simulations describe implantation into an amorphous structure<sup>2</sup>. The crystalline structure of Si is properly taken into account in crystalline-BCA methods<sup>3-6</sup>. Due to the fact that the collisions of atoms are approximated to be binary collisions, the method is most reliable in the high energy regime<sup>7</sup>. The simulations with the BCA methods are very fast due to the approximations used. The advantages of the MD method<sup>8,9</sup> are the lack of free parameters and the accuracy in many-body-collisions needed in the low energy regime ( $\leq$  keV region). On the other hand the MD simulations are slower than the BCA ones.

Different approximation methods have been utilized

to make the MD method reliable to calculate also implantation profiles for low energy implantations<sup>9,10</sup>. The use of only near neighbors of the implanted ions inside a threshold volume (simulation box) brings the calculation times close to those of BCA. This method has been included in the MDRANGE<sup>8</sup> code developed by our group. The present model is based on that.

The paper is organized as follows: In section II, we present the basic features of the MDRANGE. Section IIA presents the electronic stopping model used in our model, and the new damage model is explained in sections IIB and IIC. In section III we present the simulation results for different ion species, discussing and summarizing these in sections IV and V, respectively.

### II. MODEL

The MDRANGE code was developed for calculating range profiles of different ion species implanted into crystalline materials in the low energy regime of 1 - 100 keV (Ref. 8). An impinging ion is followed inside a target material until it stops. The range profile histogram of ions is updated using the information of the trajectory of the current ion. The ion can be implanted in any lattice direction, and the number of simulated ions is typically between 10000 - 20000, which is enough to achieve reliable statistics in the histogram.

The atomic interactions are calculated with MD methods<sup>11</sup>. The model uses repulsive pair-potentials obtained by density-functional methods<sup>12-14</sup> for calculating the elastic scattering of the implanted ion. The interatomic potentials used have been intensively tested<sup>15</sup>. Possible disagreements with experiments at low doses are most likely due to inaccuracies in the electronic stopping in sample structures.

The forces affecting the ion are calculated only inside a

simulation box surrounding the ion. The dimensions are defined by unit cell multipliers. In this work we selected a box made of  $4 \times 4 \times 4$  Si unit cells, each with an initial side length of 5.43 Å. A simulation box contains 512 Si atoms. The simulation box travels with the ion. The atom positions are updated every time the ion comes closer to the border of the box than the thickness of one unit cell (5.43 Å). When the simulation box is updated, the layer that is copied to the box can be altered as a function of depth, making it possible to simulate multi-layered structures.

The calculations of the forces between a recoil ion and target atoms are done only inside the simulation cell. The target atoms do not interact with each other (recoil interaction approximation (RIA)). If they are moved outside of the simulation cell, the information about them is lost. This method has been found to be valid for calculating range profiles without losing accuracy. The method is explained in details elsewhere<sup>16</sup>.

The material in which the ion moves can be constructed from any crystalline or amorphous layer, for which a small periodic box with atom coordinates can be constructed. For multi-layered targets, the simulation box has the same size for all the layers.

### A. Electronic stopping

The electronic stopping power used in our model is based on the density-functional calculations of Echenique *et al.*<sup>17–19</sup>. It takes into account the electron cloud of an implanted ion. Scaling laws are not employed. The electronic stopping of an ion moving with velocity  $v$  much lower than the Fermi velocity of the electrons of a material can be expressed as<sup>20,21</sup>

$$S_e = \frac{3v}{k_F r_s^3} \sum_{l=0}^{\infty} (l+1) \sin^2(\delta_l(E_F) - \delta_{l+1}(E_F)), \quad (1)$$

where  $k_F$  is the Fermi momentum of the electrons of a target atom,  $r_s$  the one-electron radius ( $r_s = (3 / (4 \pi \rho))^{1/3}$ , where  $\rho$  is the electron density) and  $\delta_l(E_F)$  the phase shift for the scattering of an electron at the Fermi energy. The phase shifts are calculated separately for a given ion and regular grid of  $r_s$  values. The tabulated values are then interpolated for a desired electron density used in the program.

In the previous version of our code<sup>22</sup>, the electron density of the Si atoms was obtained very accurately from a precalculated three-dimensional charge distribution table. The method demands a static structure and thus can not be directly used in the current damage build-up model. Instead we calculate the electron density by assuming a point-like ion and a spherical symmetric electron distribution<sup>2</sup> of atoms in a material and summing the densities over the nearest atoms of the ion inside a sphere with a radius of 1.47 Å. This method is local and takes into account the lower electron density in channels. The approximation leads to some inaccuracies in the handling of the channeling phenomena<sup>23</sup>. For compound materials (for example surface oxide), the electronic stopping is calculated using the ZBL model<sup>2</sup>.

### B. Damage build-up modeling

The method of selecting simulation boxes along with the ion trajectory makes it possible to combine the changes in the amorphization state of a target with the slowing down calculations.

When an ion moves inside a material, it loses kinetic energy in collisions with atoms and interactions with electrons. The energy  $F_D$  deposited in elastic collisions with atoms is mainly responsible for the damage produced in the target material at keV energies. The amorphization of the material is described by choosing the updated atom coordinates from 20 pre-damaged boxes. The choice of a box is done according to the amount of nuclear deposited energy  $F_D$  left by previous ions in the depth regime where the updating needs to be done.

The amount of damage is dose-dependent. For high doses ( $\gtrsim 1 \times 10^{14}$  ions/cm<sup>2</sup>) the implanted region of the target material gets amorphized. The damage blocks channels and causes strong dechanneling of ions. Consequently the range profile changes shape towards the profile of a totally amorphous material.

In our model  $F_D$  is the nuclear energy deposited to primary knock-on atoms by the recoil ion. We can calculate  $F_D$  as a function of depth  $z$  and number of implanted ions  $n$  for the material.  $n$  grows from 0 to  $n_{max}$ , where  $n_{max}$  is the total number of ions to be simulated. The deposited dose  $D(z, n)$  (eV/atom) corresponding to an experimental value is calculated as

$$D(z, n) = F_D(z, n) \times S, \quad (2)$$

where  $S = (D_{exp}(\text{ions/cm}^2)/D_{sim}(\text{ions/cm}^2))$ . This factor links the experimental dose of ions to the dose of ions used for precalculated damage in the simulation.

The depth  $z$  for an implanted dose is defined in steps of unit cells, i.e. as the energy deposited in nuclear collisions to 5.43 Å thick layers inside the material. When the ion comes close to the border of a simulation box at a certain depth, the damage accumulated to the unit cell in front of the ion is checked, and the amorphization box with the right amount of damage is selected for the simulation. The procedure is illustrated in Fig. 1. In this way the model takes into account the cumulative damage build-up process without free parameters and probabilities.

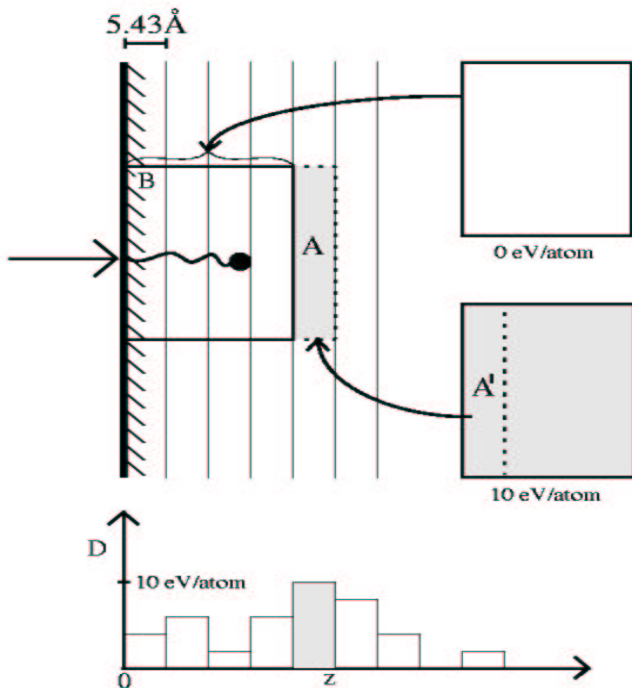


FIG. 1. Sketch of the simulation boxes along with the ion trajectory. The ion is surrounded by a simulation box. It has a side length of 4 unit cells ( $4 \times 5.43 \text{ \AA}$ ) and originally corresponds to a crystalline box without damage. For an ion close to the border of the simulation box, the dose (eV/atom) is checked for the next layer (layer A in the picture) from the D-function of eq. (2). If the dose in the layer A is 10 eV/atom, a layer with the same dose is copied to the simulation box from the predamaged box (A'). The layer at the surface (B) is discarded at the same time, i.e. the simulation box has moved a step of 5.43 Å.

### C. Choosing the amorphous simulation boxes

Nord *et al.*<sup>7</sup> have employed MD to study the amorphization mechanism and effect of different many-body-potentials on the amorphization process in silicon. They started the amorphization simulation with a simulation cell of  $17 \times 17 \times 17$  unit boxes of perfect silicon crystal. Periodic boundary conditions were used. The cell was then bombarded with low-energy (3 eV - 2 keV) recoils in random places according to a pre-calculated primary recoil spectrum. This was continued until the cell was totally amorphous. Between successive recoils the cell was relaxed to zero temperature and average zero pressure. The positions of atoms were stored. This resulted in cells with different amorphization doses (eV/atom). We now chose 20 different cells with constant dose increment in the region from 0 to 14.3 eV/atom. The final value corresponds to a completely amorphous structure and the amorphization dose is in close agreement with experiments. We chose cells for which the Tersoff-III<sup>24</sup> potential was used.

Because we needed relatively small simulation boxes compared to the amorphization cells, we calculated the

average potential energy of atoms for volumes of  $4 \times 4 \times 4$  unit cells based on amorphization volumes of the  $17 \times 17 \times 17$  unit cells and compared it to the average potential energy of the whole cell. We then chose the  $4 \times 4 \times 4$  volumes that had the potential energy closest to the average value. The number of atoms in the chosen simulation box had to be close ( $\pm 2\%$ ) to the number of atoms in the perfect crystal (512 atoms). The channels in the simulation boxes of different amorphization states were matched to each others. Since the volume of the unit cell increases along with the amorphization state, the boxes had to be scaled into the same volume in the selection phase in order to keep the channel match. During the actual range calculation, the atom coordinates in a simulation box were scaled to match the original dimensions of the amorphization box that is being copied into the range simulation box. In this way the program could also scale the path of the implanted ion when it is moving inside different simulation boxes, so that the ions moving in the channels do not get dechanneled because of volume changes during the advance.

## III. RESULTS OF SIMULATIONS

In the simulations, initially crystalline silicon was used as a target material. A native amorphous oxide layer on the surface was taken into account, if it was reported experimentally. An oxide layer of 16.29 Å was assumed, if no information was available. The surface temperature of the experiments, 300 K, was used and realistic atomic thermal displacements were obtained by setting the Debye temperature of silicon to 519 K (Ref. 10). A beam divergence of  $1^\circ$  was used in all simulations. The number of simulated ions was varied between 10000 and 30000, but no significant difference was observed in the statistical variation of the profile. Implantations in a random direction (off any channeling axis) were done in simulations by tilting the azimuthal angle of the implantation direction by 6 - 8 degrees away from the  $\langle 100 \rangle$  surface normal.

Effects of the damage build-up on the range profiles are illustrated in Figs. 2 and 3 for ions impinging the sample in the random and channeling direction, respectively. It can be seen that in both cases the accumulated damage strongly affects the range profile.

The simulations illustrated in the subsections A - D were chosen to show both representative examples and problematic cases. We emphasize that we include the most problematic cases of all of our simulations.

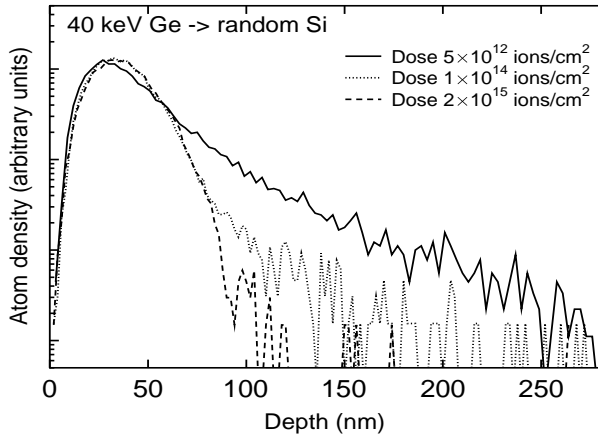


FIG. 2. Effect of the damage build-up to the simulated random direction implantation profiles of 40 keV Ge. The peaks are scaled to the same value.

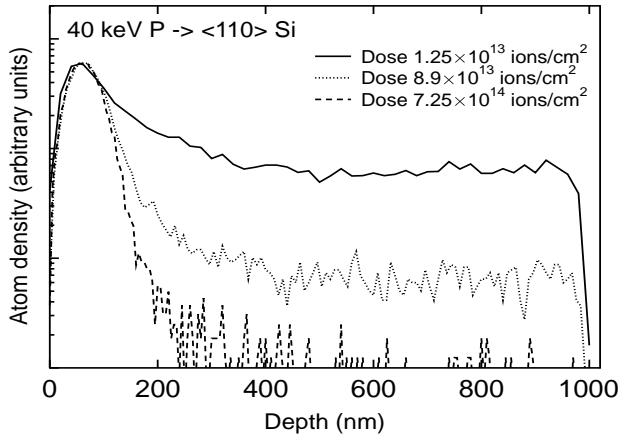


FIG. 3. Effect of the damage build-up to the simulated channeling direction implantation profiles of 40 keV P. The peaks are scaled to the same value.

### A. Germanium implantations

Ge implantations were first simulated for 40 and 80 keV ions impinging in the random direction. This was done due to the high value of the nuclear stopping compared to the electronic one. The nuclear stopping accounts for 70 - 90 % of the energy loss. This enables us to check the effects of the amorphization model without significant uncertainties arising from the electronic stopping and channeling effects. No oxide layer was assumed to be at the surface due to the HF dip done in the experiments<sup>25</sup>.

Figure 4 shows the simulated results compared with experimental data<sup>25</sup> of 40 keV implantations in the random direction for doses varying from  $5 \times 10^{12}$  to  $2 \times 10^{15}$  ions/cm<sup>2</sup>. Our model predicts quite accurately the range profiles. The tails of the profiles are slightly overestimated in the two low-dose cases. In Fig. 5 the implantation of 80 keV Ge ions in the channeling direction  $\langle 100 \rangle$  to a dose of  $1 \times 10^{14}$  ions/cm<sup>2</sup> is compared with the implantation to the random direction. We can see that the tail of the  $\langle 100 \rangle$  profile is overestimated and the peak is too sharp. A possible

reason for the peak can be directly seen from the damage profile in Fig. 6. A clearly too high amorphization state occurs in the simulations. The problem with the tail is probably linked to the shortcomings of the electronic stopping model.

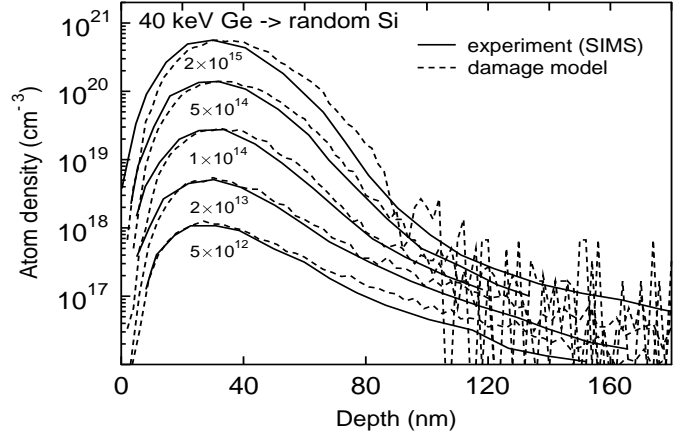


FIG. 4. Simulated and measured<sup>25</sup> ranges of 40 keV Ge ions in the random direction of crystalline silicon with different doses (in ions/cm<sup>2</sup>).

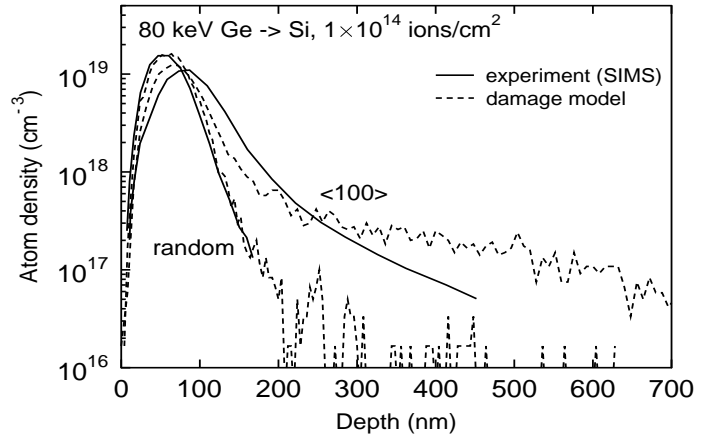


FIG. 5. Simulated and measured<sup>25</sup> ranges of 80 keV Ge ions in the random direction and  $\langle 100 \rangle$  channel of silicon.

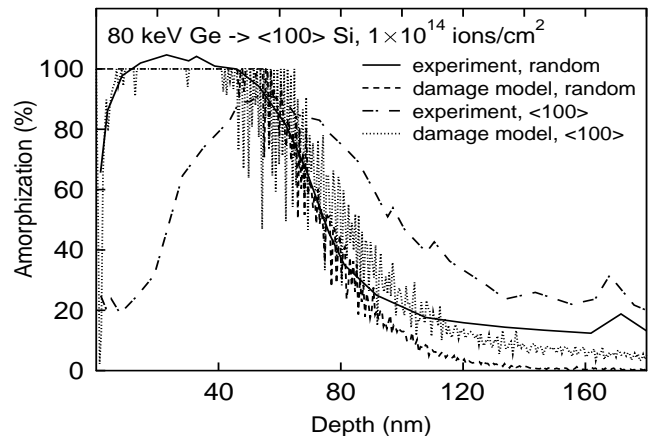


FIG. 6. Simulated and measured<sup>25</sup> percentage of amorphization as a function of depth for 80 keV Ge ions in the random direction and the  $\langle 100 \rangle$  channel of silicon. The overestimation of the amorphization can be seen for the prediction in the channeling case.

## B. Boron implantations

We simulated boron implantation profiles for 15 keV ions in the random direction and  $\langle 100 \rangle$  channel for doses ranging from  $1 \times 10^{13}$  to  $8 \times 10^{15}$  ions/cm<sup>2</sup>. A 16.29 Å thick layer of oxide at the surface was assumed. Figure 7 shows that the model predicts the random cases quite accurately. Figure 8 shows that channels are blocked slightly too much in the simulations for the medium dose ( $5 \times 10^{14}$  ions/cm<sup>2</sup>) profile, depth region 100 to 200 nm. The overestimation of the tails in the  $\langle 100 \rangle$  channels is due to the use of spherically symmetric electron densities in the electronic stopping model. It can be corrected by using three dimensional electron densities<sup>22</sup>.

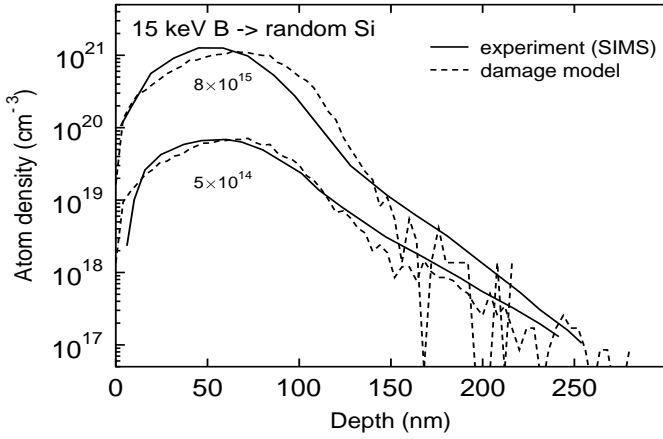


FIG. 7. Simulated and measured<sup>26</sup> ranges of 15 keV B ions in the random direction of silicon for different doses (in ions/cm<sup>2</sup>).

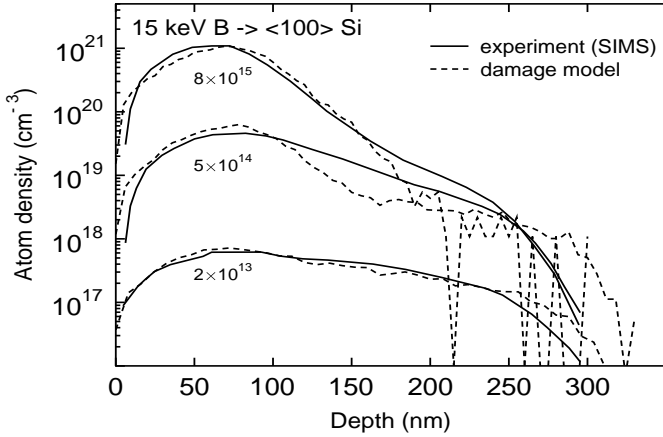


FIG. 8. Simulated and measured<sup>26</sup> ranges of 15 keV B ions in the  $\langle 100 \rangle$  direction of silicon for different doses (in ions/cm<sup>2</sup>).

## C. Phosphorus implantations

In Fig. 9 we can see the result of the simulations of the 40 keV P ion implantations in the  $\langle 110 \rangle$  direction for doses of  $1.2 \times 10^{13}$ ,  $8.9 \times 10^{13}$  and  $7.25 \times 10^{14}$  ions/cm<sup>2</sup>. A 16.29 Å thick layer of oxide was assumed in the simulations. There is a small disagreement in the peak position compared to the experiments<sup>27</sup>. The overall

agreement of the profiles is good. Unfortunately a detailed description of the experiments is not given in Ref. 27. Thus the simulation parameters can be different from the experiments and could explain the differences in the peak position of the profiles. The overestimation of the tails is due to problems in the electronic stopping model in the  $\langle 110 \rangle$  channel<sup>22</sup> and is not related to the damage build-up model.

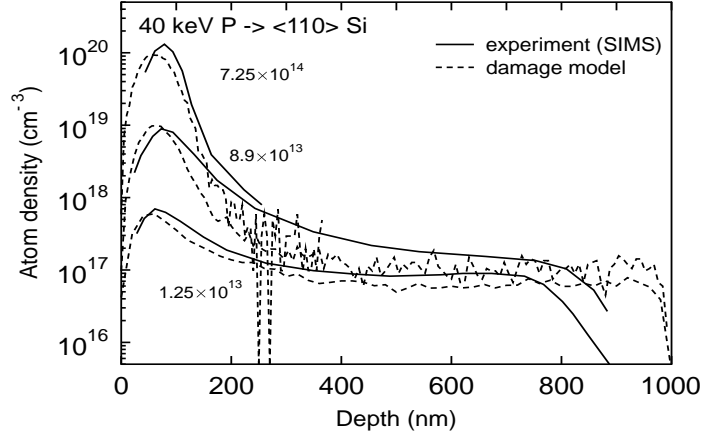


FIG. 9. Simulated and measured<sup>27</sup> ranges of 40 keV P ions in the  $\langle 110 \rangle$  direction of silicon for different doses (in ions/cm<sup>2</sup>).

## D. Indium implantations

The simulations for indium were made to test the model for heavier ions. We simulated implantation of 50 and 100 keV In ions in the  $\langle 100 \rangle$  direction for doses of  $2 \times 10^{12}$  and  $2 \times 10^{14}$  ions/cm<sup>2</sup>. The comparison to the experiments<sup>25</sup> is shown in Figs. 10 and 11. No surface oxide was used in the simulations due to the HF dipping used in the experiments<sup>25</sup>. Our model predicts well the peaks of the high dose profiles in the amorphous material, but overestimates the tails in the 50 keV case. The amorphization state is quite well predicted in comparison with the RBS measurements<sup>25</sup>, as can be seen in Fig 12.

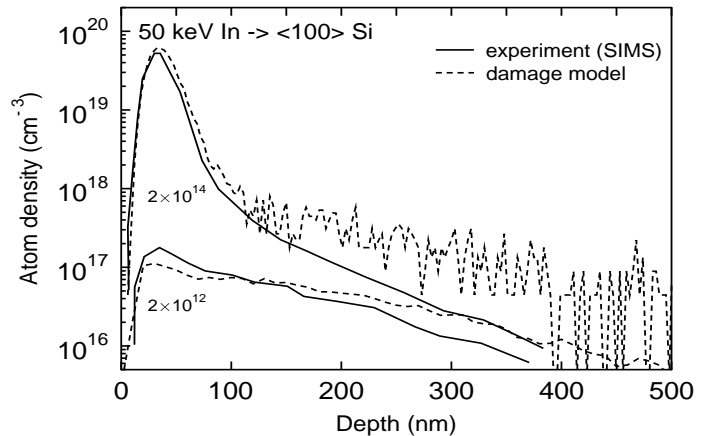


FIG. 10. Simulated and measured<sup>25</sup> ranges of 50 keV In ions in the  $\langle 100 \rangle$  direction of silicon for different doses (in ions/cm<sup>2</sup>).

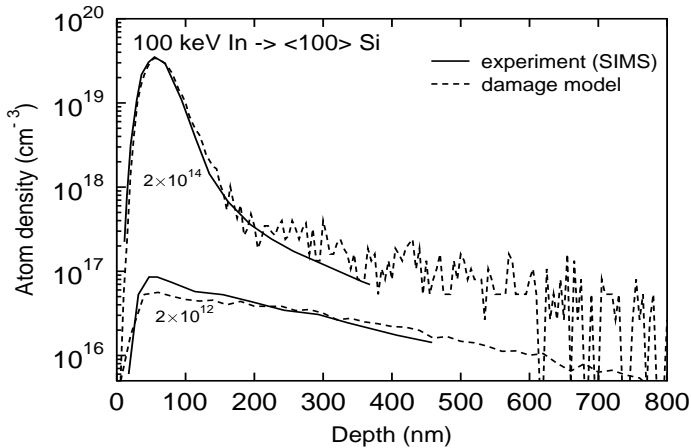


FIG. 11. Simulated and measured<sup>25</sup> ranges of 100 keV In ions in the  $\langle 100 \rangle$  direction of silicon for different doses (in ions/cm<sup>2</sup>).

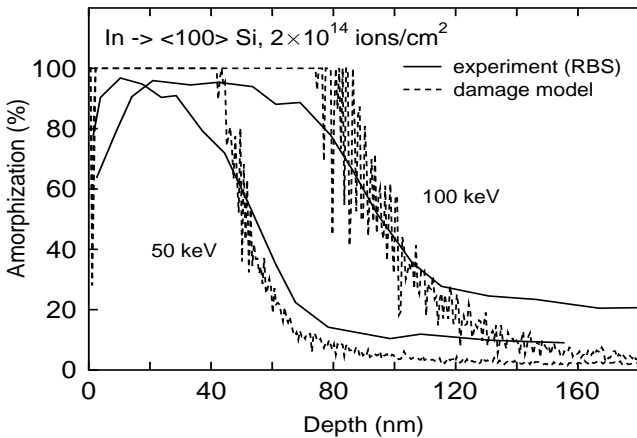


FIG. 12. Simulated and measured<sup>25</sup> percentage of amorphization as a function of depth of 50 and 100 keV In ions in the  $\langle 100 \rangle$  direction of silicon.

#### IV. DISCUSSION

We have presented results of our damage build-up model for dose-dependent range profiles in crystalline Si, and found a very good agreement with experiments. There are, however, a few remaining discrepancies. We will now examine a few possible reasons for these. We first study with simulations how much the results are affected by sputtering and the approximation that the deposited energy is distributed only in a very narrow region. After this, we discuss other possible sources of errors.

##### A. Sputtering

There is a clear difference in the simulated and experimental range profiles of high dose implantations of Ge in the random direction (Fig. 4) near the surface. We tested if this could be explained and corrected in the simulations by taking the sputtering process into account.

When the implantation dose gets high, the surface which is under bombardment starts to experience a surface erosion. The ejection of particles from the surface, namely the sputtering, affects the range profiles by shifting the profiles towards the surface, because the measurements are done from the eroded surface after the implantation. In the linear-collision-cascade regime the most commonly used theory of sputtering is the one by Sigmund<sup>28</sup>. The linearity means that the number of recoils is proportional to the nuclear energy deposited per unit length. We can express the sputtering yield  $Y$  for particles incident normal to the surface as<sup>29</sup>

$$Y \cong 0.042(\text{\AA})^{-2} * \frac{F_D}{N * U_0}, \quad (3)$$

where  $N$  is the atomic density in  $(\text{\AA})^{-3}$  and  $U_0$  is the surface binding energy in eV and  $F_D$  is the nuclear deposited energy per unit length in the surface. This equation has been found to be in good agreement with experiments, when thermal spikes are not present.

In the simulations we used a surface binding energy of 4.63 eV for Si atoms and calculated  $F_D$  as in our damage build-up model, but using the average value in the depth of the unit cell ( $F_D(\text{surfacerlayer})/5.43\text{\AA}$ ). The eroded amount of surface was calculated from eq. (3) after each implanted ion. The initial surface atoms which were inside the eroded volume were then removed before the next ion was implanted. The thickness of the eroded surface layer was subtracted from the range profile after each ion. The final range profile was thus comparable with the measured profile.

The comparison of the simulated profiles (obtained with and without sputtering) with the experiment<sup>25</sup> is illustrated in Fig. 13, for the implantation of 40 keV Ge in the random direction for doses of  $2 \times 10^{13}$  and  $2 \times 10^{15}$  ions/cm<sup>2</sup>. It can be seen that the effect of the sputtering can explain the shift in the peak position towards the surface. In these simulations the sputtering yields are over 20 atoms/ion in the sputtering model, which is over twice the amount the experiments suggest<sup>29</sup>. On the other hand, due to thermal spikes and surface roughening the sputtering yield can get much higher than the values obtained from Sigmund's linear theory<sup>30</sup>. Thus our model is probably closer to the experimental values than the linear theory, even though we use just the linear sputtering theory.

In the simulations of high dose implantation of B, In and P the effect of the sputtering modeling was similar to the Ge implantation (Fig. 13) but the effect was small. Hence sputtering can not explain the other discrepancies observed.

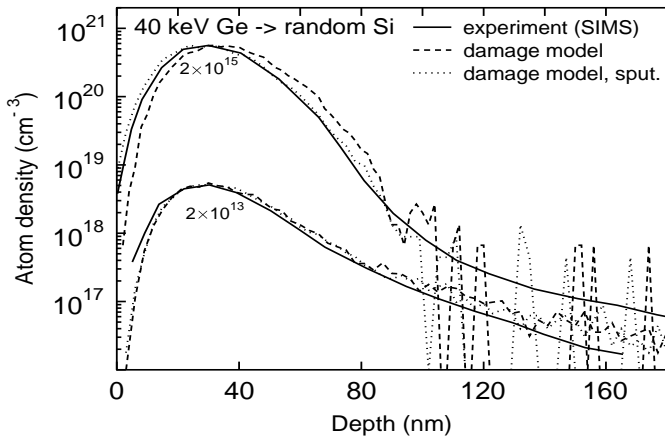


FIG. 13. Simulated and measured<sup>25</sup> ranges of 40 keV Ge ions in the random direction of silicon for doses of  $2 \times 10^{13}$  and  $2 \times 10^{15}$  ions/cm<sup>2</sup>. The simulations have been done with the damage model without and with (sput.) the sputtering model.

### B. Locality of damage deposition

We note that to speed up the calculations the full collision calculation is done only between the colliding ion and target atoms inside the current simulation cell. We do not keep track of the target atoms when they are no longer inside the simulation cell, nor calculate the interactions between them. This causes some uncertainties to the exact locations where the deposited energy has accumulated. This is a problem when small-angle collisions happen and the transfer of the nuclear deposited energy is high. Normally a large sudden change in energy is transferred to the environment in collision cascades, but in our model the energy is supposed to stay in the layer where the collision has taken place. In other words, one collision can in extreme cases totally amorphize the whole thin (5.43Å) simulation layer.

In implantations in the channeling directions the locality of  $F_D$  closes the channels too fast in the volume near the surface. This results in too strong dechanneling of the next ions. At the same time the volume below that region does not amorphize almost at all and the tail of the profile is overestimated. The explanation is that the knocked target atoms from the primary collisions with the ion can be channeled as well, causing damage in the deeper areas of the material also<sup>31</sup>.

These effects can be seen from the range profile of 80 keV Ge ions (Fig. 5), where the random case shows clearly better agreement with the experiments than the channeling case, which has a clearly too strong amorphous effect in the peak. In a work based on UT-MARLOWE<sup>25</sup>, this problem has been solved by introducing a cut-off value for the transferred energy that is taken into account in the damage state calculation. If the energy transfer is above the cut-off value, only the cut-off energy is used in the calculation. Because we do not want to include a free parameter depending on the ion species, the cut-off value was not included in our model.

Some test simulations were done where the nuclear

deposited energy was distributed into the environment with a Gaussian distribution after a collision event. We simulated the nuclear deposited energy distributions and the range profiles of random implantations of Si into Si with energies varying from 100 eV to 100 keV. We then approximated that the damage distributions are half-Gaussian, so that the peak of the distribution is in the place where the collision of the atoms took place and  $F_D$  is distributed only away from the surface. The straggle of the distribution was taken from the straggle values of range profiles of the simulations where Si ions were implanted into Si in random direction. In these simulations the range profiles are smoother than the deposited energy distributions, and they have approximately the same form. This method did not affect the range profiles much in the random cases nor the channeling cases. The exception was the 80 keV germanium implantation in the  $\langle 100 \rangle$  direction, where we obtained better agreement with the experiments because the amorphization percentage as a function of depth was very well predicted compared with the experiment. Overall the amorphization percentage profiles were shifted deeper in, making the agreement with the experiments slightly worse in the random implantation cases for higher energies and better for lower energies. Thus no consistent improvement was observed and the improvement for Ge may have been fortuitous.

### C. Other sources of uncertainty

In the tests described in the preceding two subsections, we found that sputtering can clearly in some cases of very high dose implantation explain some of the discrepancy with experiments, while the spread out damage deposition model could not conclusively remove the remaining discrepancies.

One possible source of discrepancy which remains is the recombination of damage. We have checked the recoil spectrum for 80 keV Ge implantations in the random and  $\langle 100 \rangle$  directions. The number of ions transferring energy to atoms is higher in the low-energy end in the channel direction than in the random direction. For example, there are 3 times more 1 keV recoils in the random direction than in the channeling direction. This means that in the channeling case, there are more defects (Frenkel pairs) produced by low-energy recoils. These are mostly annealed during the implantation<sup>32-35</sup>, leaving less stable damage to the crystal than our model suggests. In the random case the damage is more clusterized and stable. This explains why the amorphization states predicted by our model are more compatible with the experiments in the simulations of random direction implantations (see Fig. 6).

Since it is very difficult and computationally expensive to handle damage recombination<sup>36,37</sup>, we can not predict this effect during the simulations. But this is an important factor in some of the channeling implantations.

One reason which clearly does explain some of the discrepancies in the channeling tails is the electronic stopping model used. We know from a previous study

comparing spherically symmetric and three-dimensional electron distributions<sup>22</sup> that there are some minor problems associated with the former, which leads to errors in the channels. This could be corrected for by calculating a three-dimensional total electron density in each of the 20 simulation cells with different degrees of amorphization. Unfortunately calculating the total (as opposed to valence electron only) charge distribution is very complicated, and hence was not carried out as part of this work.

The low statistics in the tails of the profiles is a minor numerical problem and we would like to mention that the REED<sup>9,38</sup> model could be incorporated into the model if the tails of the range profiles are of special interest.

Finally, we mention that one likely source of discrepancy may be minor errors in the experimental distributions themselves. In the SIMS measurements, the depth scale is obtained from the sputtering rate, which normally is assumed to be constant throughout the measurement. However, in some of the cases we compare with, the density of impurity atoms is several atomic %. Thus the sputtering rate in these cases can be dependent on the depth, which could introduce an error source in the depth scale.

## V. CONCLUSIONS

We have developed a new method for predicting dose-dependent range profiles in Si with molecular dynamical methods and without bringing any free parameters or losing the efficiency of the simulation. Previously calculated data on the amorphization of crystalline silicon was used to obtain silicon structures at different degrees of amorphization. The comparisons with the experiments show very good agreement for implantations in the random direction and good overall agreement in the channeling cases.

## ACKNOWLEDGMENTS

We thank M.Sc. J. Nord for giving data from his amorphization simulations to our disposal. The research was supported by the Academy of Finland under projects No. 44215 and 46788,

<sup>1</sup> G. D. Watkins, in *Defects and Diffusion in Silicon Processing*, Vol. 469 of *MRS Symposium Proceedings*, edited by T. Diaz de la Rubia, S. Coffa, P. A. Stolk, and C. S. Rafferty (Materials Research Society, Pittsburgh, 1997), p. 139.

<sup>2</sup> J. F. Ziegler, J. P. Biersack, and U. Littmark, *The Stopping and Range of Ions in Matter* (Pergamon, New York, 1985).

<sup>3</sup> M. Hautala, *Phys. Rev. B* **30**, 5010 (1984).

<sup>4</sup> M. T. Robinson and I. M. Torrens, *Phys. Rev. B* **9**, 5008 (1974).

<sup>5</sup> Q. Yang, T. Li, B. V. King, and R. J. MacDonald, *Phys. Rev. B* **53**, 3032 (1996).

<sup>6</sup> K. M. Klein, C. Park, and A. F. Tasch, *IEEE Trans. Electron Devices* **39**, 1614 (1992).

<sup>7</sup> G. Hobler and G. Betz, *Nucl. Instr. Meth. Phys. Res. B* **180**, 203 (2001).

<sup>8</sup> K. Nordlund, *Comput. Mater. Sci.* **3**, 448 (1995).

<sup>9</sup> K. M. Beardmore and N. Grønbech-Jensen, *Phys. Rev. E* **57**, 7278 (1998).

<sup>10</sup> J. Sillanpää, K. Nordlund, and J. Keinonen, *Phys. Rev. B* **62**, 3109 (2000).

<sup>11</sup> M. P. Allen and D. J. Tildesley, *Computer Simulation of Liquids* (Oxford University Press, Oxford, England, 1989).

<sup>12</sup> R. O. Jones and O. Gunnarsson, *Rev. Mod. Phys.* **61**, 689 (1989).

<sup>13</sup> J. Keinonen, A. Kuronen, K. Nordlund, R. M. Nieminen, and A. P. Seitsonen, *Nucl. Instr. Meth. Phys. Res. B* **88**, 382 (1994).

<sup>14</sup> J. Delley, *J. Chem. Phys.* **92**, 508 (1990).

<sup>15</sup> K. Nordlund, N. Runeberg, and D. Sundholm, *Nucl. Instr. Meth. Phys. Res. B* **132**, 45 (1997).

<sup>16</sup> K. Nordlund, *Acta Polytechnica Scandinavica, Applied Physics Series* **202**, 1 (1995), PhD thesis, University of Helsinki.

<sup>17</sup> M. J. Puska and R. M. Nieminen, *Phys. Rev. B* **27**, 6121 (1983).

<sup>18</sup> P. M. Echenique, R. M. Nieminen, and R. H. Ritchie, *Solid State Comm.* **37**, 779 (1981).

<sup>19</sup> P. M. Echenique, R. M. Nieminen, J. C. Ashley, and R. H. Ritchie, *Phys. Rev. A* **33**, 897 (1986).

<sup>20</sup> J. Finneman, dissertation, The Institute of Physics, Aarhus, 1968 (unpublished).

<sup>21</sup> T. L. Ferrell and R. H. Ritchie, *Phys. Rev. B* **16**, 115 (1977).

<sup>22</sup> J. Sillanpää, J. Peltola, K. Nordlund, J. Keinonen, and M. J. Puska, *Phys. Rev. B* (2000), accepted for publication.

<sup>23</sup> D. Cai, N. Grønbech-Jensen, C. M. Snell, and K. M. Beardmore, *Phys. Rev. B* **54**, 17147 (1996).

<sup>24</sup> J. Tersoff, *Phys. Rev. B* **38**, 9902 (1988).

<sup>25</sup> Y. Chen, B. Obradovic, M. Morris, and G. W. et al, (1999).

<sup>26</sup> K. M. Klein, C. Park, and A. F. Tasch, *Nucl. Instr. Meth. Phys. Res. B* **59**, (1991).

<sup>27</sup> G. Dearnaley, J. H. Freeman, G. A. Gard, and M. A. Wilkins, *Canadian Journal of Physics* **46**, 587 (1967).

<sup>28</sup> P. Sigmund, *Phys. Rev.* **184**, 383 (1969).

<sup>29</sup> M. Nastasi, J. Mayer, and J. Hirvonen, *Ion-Solid Interactions - Fundamentals and Applications* (Cambridge University Press, Cambridge, Great Britain, 1996).

<sup>30</sup> M. Urbassek and P. Sigmund, *Appl. Phys. A* **35**, 19 (1984).

<sup>31</sup> R. Chakarova and I. Pazsit, *Nucl. Instr. Meth. Phys. Res. B* **164**, (2000).

<sup>32</sup> P. Ehrhart and H. Zillgen, in *Defects and Diffusion in Silicon Processing*, Vol. 469 of *MRS Symposium Proceedings*, edited by T. Diaz de la Rubia, S. Coffa, P. A. Stolk, and C. S. Rafferty (Materials Research Society, Pittsburgh, 1997), p. 175.

<sup>33</sup> H. Zillgen and P. Ehrhart, *Nucl. Instr. Meth. Phys. Res. B* **127-128**, 27 (1996).

<sup>34</sup> K. Kyuno, D. C. Cahill, R. S. Averback, J. Tarus, and K. Nordlund, *Phys. Rev. Lett.* **83**, 4788 (1999).

<sup>35</sup> P. Partyka, Y. Zhong, K. Nordlund, R. S. Averback, I. K. Robinson, and P. Ehrhart, *Phys. Rev. B* (2000), submitted for publication.

<sup>36</sup> M. Jaraiz, G. H. Gilmer, J. M. Poate, and T. Diaz de la Rubia, *Appl. Phys. Lett.* **68**, 409 (1996).

- <sup>37</sup> H. L. Heinisch, B. N. Singh, and T. Diaz de la Rubia, J. Nucl. Mat. **212-215**, 127 (1994).
- <sup>38</sup> J. M. Hernandez-Mangas, J. Arias, M. Jaraiz, L. Bailon, and J. Barbolla, Nucl. Instr. Meth. Phys. Res. B **174**, 433 (2001).